Climatic Change (2008) 87 (Suppl 1):S273–S292
DOI 10.1007/s10584-007-9351-3

A preliminary assessment of the sensitivity of air quality in California to global change

Michael J. Kleeman

Received: 2 August 2006 / Accepted: 5 October 2007 / Published online: 8 December 2007

Abstract A regional air quality model was used to quantify the effect of temperature, humidity, mixing depth, and background concentrations on ozone (O_3) and airborne particulate matter during three air quality episodes in California. Increasing temperature with no change in absolute humidity promoted the formation of O_3 by +2 to +9 ppb K^{-1} through increased reaction rates. Increasing temperature with no change in relative humidity increased predicted O_3 concentrations by +2 to +15 ppb K^{-1} through enhanced production of hydroxyl radical combined with increased reaction rates. Increasing mixing depth promoted the formation of O_3 in regions with an over-abundance of fresh NO emissions (such as central Los Angeles) by providing extra dilution. Increasing temperature with no change in absolute humidity reduced particle water content and promoted the evaporation of ammonium nitrate at a rate of −3 to −7 μg m^{-3} K^{-1}. Increasing temperature with no change in relative humidity maintained particle water content and moderated ammonium nitrate evaporation rates to a maximum value of −3 μg m^{-3} K^{-1} during warmer episodes and increased ammonium nitrate condensation by +1.5 μg m^{-3} K^{-1} during colder episodes. Increasing mixing depth reduced the concentration of primary particulate matter but increased the formation of secondary particulate matter in regions with an over-abundance of fresh NO emissions. O_3 transported into California from upwind areas enhanced the formation of particulate nitrate by promoting the formation of N_2O_5 and HNO_3 at night. A 30 ppb increase in background O_3 concentrations (roughly doubling current levels) increased maximum $PM_{2.5}$ concentrations by +7 to +16 μg m^{-3} even when temperature was simultaneously increased by +5 K with no change in absolute humidity (most unfavorable conditions for nitrate formation).

1 Introduction

California's combination of large urban populations situated in confined air basins that are subject to severe air pollution events causes significant public health concerns. Ozone (O_3)

M. J. Kleeman (✉)
Department of Civil and Environmental Engineering, University of California Davis,
Davis, CA 95616, USA
e-mail: mjKleeman@ucdavis.edu

and airborne particles with diameter smaller than 2.5 μm ($PM_{2.5}$) are two of the main ingredients of the photochemical "smog" that can form when atmospheric mixing is low, causing pollutants to be trapped near the earth's surface. The South Coast Air Basin and the San Joaquin Valley in California are the two air basins with the highest "smog" concentrations in the United States and they have a combined population greater than 15M. The adverse health effects of O_3 and $PM_{2.5}$ are widely acknowledged, and reducing the concentrations of these pollutants is an important objective for the State of California.

Changes in global population, economic development, energy consumption, and technology can have consequences for air quality in California. It is generally acknowledged that global consumption of fossil fuels has changed the earth's atmosphere in a way that will lead to sustained changes in regional meteorological patterns (i.e. Climate Change) (Houghton et al. 2001). The severity of air pollution events in California is largely determined by the strength of atmospheric stagnation events that are driven by these regional-scale meteorological patterns. Thus, global change can influence air quality in California. As a second effect, atmospheric pollutants can be directly transported between countries and even between continents (VanCuren and Cahill 2002; Vingarzan 2004) leading to increased "background" concentrations for both O_3 and $PM_{2.5}$. Background concentrations currently account for approximately 33% of the National Ambient Air Quality Standard (NAAQS) for O_3 (Vingarzan 2004) and 25% of the annual-average NAAQS for $PM_{2.5}$ in California (Kim et al. 2000). Future changes in meteorology and background concentrations will influence the local actions that must be taken in California to reduce the concentration of O_3 and $PM_{2.5}$ to acceptable levels.

The purpose of this study was to investigate the sensitivity of present-day air quality in California to changes in meteorological conditions and background pollutant concentrations. Three air quality episodes were studied that span the full range of pollution conditions that commonly occur in California. The individual effect of each variable on O_3 and $PM_{2.5}$ concentrations was identified, and preliminary conclusions were made about the likely effect of global change on air quality in California.

2 Background

The relationship between climate and air quality can be studied using General Circulation Models (GCMs) coupled to chemistry calculations (see for example (Prather et al. 2003; Mickley et al. 2004; Murazaki and Hess 2006; Liao et al. 2006)). These calculations use grid cells that are larger than 1° (>100 km at mid latitudes), making them most appropriate for regional pollutants (such as O_3) in locations that do not have complex terrain (such as the eastern United States). The majority of these studies predict that O_3 concentrations will increase in the future due to a combination of factors related to climate and emissions (Prather et al. 2003). Finer spatial scales can be resolved by dynamically downscaling meteorology and coupling to a regional air quality model. Calculations for the eastern United States (Hogrefe et al. 2004) and Europe (Langner et al. 2005) generally show that climate change will have a strong influence on surface O_3 concentrations.

Simulating the relationship between climate and $PM_{2.5}$+O_3 in the western United States is difficult because the complex topography in this region results in sharper spatial gradients. A few studies have been performed to dynamically downscale meteorological predictions (Leung et al. 2004; Duffy et al. 2006) but these results have not yet been combined with chemical transport models. Perturbation studies can be used to identify the mechanistic response of pollutant concentrations to meteorological variables even when the

full dynamics of the system are not completely known. Previous studies have examined the effect of temperature change on tropospheric O_3 concentrations in the eastern U.S. (Klonecki and Levy 1997; Sillman and Samson 1995), soil moisture change on O_3 and $PM_{2.5}$ concentrations in the western U.S. (Jacobson 1999), and temperature change on O_3 and $PM_{2.5}$ concentrations in the western U.S. (Aw and Kleeman 2003). The present study will build on this previous work by conducting a rigorous sensitivity analysis of three separate air quality episodes that span the full range of conditions experienced in California.

3 Model description

The UCD-CIT air quality model is a reactive chemical transport model that predicts the concentration of primary and secondary pollutants in the gas and particle phase in the presence of emissions, transport, deposition, chemical reaction, and phase change. Model calculations are initialized with measured concentrations and then allowed to evolve according to the governing equations for the system while enforcing boundary conditions at the edges of the model domain. Table 1 summarizes the lateral boundary conditions used during the current study. Previous studies (Kleeman and Cass 2001; Held et al. 2004; Ying and Kleeman 2006; Mysliwiec and Kleeman 2002) have described the formulation of the UCD/CIT source-oriented air quality model, and so only those aspects that differ for the current project are discussed here.

3.1 SJV simulations

The gas-phase chemical mechanism used to model episodes in the SJV is based on the SAPRC90 (Carter 1990) mechanism with extensions to predict the formation of 10 semi-volatile organic compounds (Pandis et al. 1992). The partitioning of semi-volatile organic species to the particle phase is calculated using an absorption model calibrated using surrogate species that have representative properties for the 10 lumped model compounds

Table 1 Lateral boundary conditions used during model simulations

Pollutant	Lateral boundary concentration	Notes
CO	200 ppb	Interpolated value from measurements used in surface cells
CO_2	332 ppb	
SO_2	1 ppb	
NO_2	1 ppb	0 ppb used on North boundary during Sept 7–9, 1993 simulation
NO	1 ppb	0 ppb used on North boundary during Sept 7–9, 1993 simulation
O_3	30 ppb	0 ppb used on North boundary during Sept 7–9, 1993 simulation
RHC	7 ppb	0 ppb used on North boundary during Sept 7–9, 1993 simulation
HCHO/CCHO/RCHO	0–5 ppb	Exact value depends on measurements during episode
HNO_3/HCl/NH3		Interpolated from measurements during episode
PM Species		Interpolated from measurements during episode

(Odum et al. 1996). The temperature dependence of the surrogate species is estimated using the Classius Clapyron equation based on a literature survey of available thermodynamic data (Aw and Kleeman 2003).

3.2 SoCAB simulations

The Caltech Atmospheric Chemistry Model (CACM) (Griffin et al. 2002a, 2005) was integrated into the UCD/CIT framework with several modifications. Ethane was tracked as an individual species so that an appropriate rate constant could be specified for reaction with hydroxyl radical. The thermodynamic data describing the equilibrium concentration of semi-volatile reaction products above the condensed aqueous phase (Griffin et al. 2005; Pun et al. 2002) was adapted to work with the dynamic (non-equilibrium) treatment used in the UCD/CIT air quality model. A single subroutine was created to dynamically partition inorganic and organic species between the gas and particle phases. The method of Kusik and Meissner (1978) was used to predict activity coefficients for inorganic species while the UNIFAC model (Fredenslund et al. 1977) was used to predict activity coefficients for organic species. The vapor pressure of water above the particle surface was adjusted to account for organic and inorganic solutes. Water exchange between the gas and liquid phases was calculated as a dynamic process using equations described by Kleeman et al. (1997).

4 Model application

Calculations were performed for the air pollution episodes that occurred in the South Coast Air Basin (SoCAB) on September 7–9, 1993, in the SoCAB on September 23–25, 1996, and in the San Joaquin Valley (SJV) on January 4–6, 1996. The extensive meteorological, emissions, and air quality information needed to support detailed modeling of each episode has been assembled previously, and base-case modeling studies have validated the performance of air quality models used to simulate the formation of pollutant concentrations (Kleeman and Cass 2001; Held et al. 2004; Ying and Kleeman 2006; Mysliwiec and Kleeman 2002; Fraser et al. 2000; Griffin et al. 2002b; Ying and Kleeman 2007; Held et al. 2005; Kleeman et al. 1999). Table 2 summarizes the focus pollutants used in each episode and the published studies describing those episodes. Table 3 summarizes

Table 2 Air quality episodes to be studied with sensitivity analysis

		Location	
		SoCAB	SJV
Focus Pollutant	O_3	Date: September 7–9, 1993 References: (Fraser et al. 2000; Griffin et al. 2002b)	[a]
	PM	Date: September 23–25, 1996 References: (Kleeman and Cass 2001; Mysliwiec and Kleeman 2002; Kleeman et al. 1999)	Date: January 3–5, 1996 References: (Held et al. 2004; Ying and Kleeman 2006; Held et al. 2005; Kleeman et al. 2005)

[a] Sensitivity analysis of O_3 response to climate change in the SJV is being conducted as part of a separate project funded by the US EPA at UC Berkeley.

Table 3 Emissions summary for the air quality episodes described in Table 2

	NO*x* (tons day^{-1})	VOC (tons day^{-1})	PM10 (tons day^{-1})
SoCAB Sept 7, 1993	1,066	1,828	529
SoCAB Sept 23, 1996	929	1219	381
SJV, Jan 6, 1996	526	447	187

the total emissions of oxides of nitrogen (NO*x*), volatile organic compounds (VOC), and particles with diameter smaller than 10 μm (PM_{10}) within the SoCAB and SJV during each air pollution episode.

SoCAB September 7–9, 1993 Daytime surface temperatures exceeded 35°C at inland locations and a strong elevated temperature inversion formed. Light surface winds followed the land-sea breeze pattern with onshore flow during the day and stagnation at night. Upper level winds originated from the north–north west of the modeling domain (over land). Measured O_3 concentrations exceeded 250 ppb, while 3-h average $PM_{2.5}$ concentrations reached 90 μg m^{-3}.

SoCAB September 23–25, 1996 Temperatures at inland locations were moderate with peak daytime values reaching 25°C. Winds were light onshore during the day and stagnant during the evening. The total time required for air parcels to traverse the study region from west to east was calculated to be greater than 3 days. Peak O_3 concentrations were generally less than 100 ppb while $PM_{2.5}$ concentrations measured at Riverside between the hours of 14:00–17:00 PST exceeded 75 μg m^{-3}.

SJV January 4–6, 1996 Temperatures ranged between 0°C at night to 10–15°C during the day. O_3 concentrations were less than 40 ppb, reflecting the low photochemical activity during winter pollution events in the SJV. Regional particulate nitrate concentrations built up to high levels during the stagnation event. Local emissions of carbonaceous aerosol also develop around urban areas. Measured PM_{10} concentrations during the episode reached 150 μg m^{-3} during the evening hours, with the majority of that material in the $PM_{2.5}$ size range.

Perturbations Temperature perturbations +2K and +5K were considered during the sensitivity analysis (air temperature only, ground temperature and sea surface temperature are not used in the simulation). These values span the range of IPCC projections for global mean surface temperature rise over the next 100 years. Humidity perturbations were coordinated with temperature to avoid artificially specifying an atmosphere with RH> 100%. Each temperature perturbation was evaluated once with no change to absolute humidity and once with no change to relative humidity. Perturbations in mixing depth considered in this study were chosen to be +50%. Mixing depth perturbations were carried out without changes to air temperature even though this is a highly artificial case. The sensitivity to mixing depth by itself reveals the effect of dilution separately from the effect of temperature on reaction rates.

Perturbations to wind speed were not considered in the present study. Although wind speed is expected to change in concert with other meteorological parameters, the appropriate direction and level of perturbation is not obvious. One recent study suggests

that higher soil moisture content leads to decreased wind speed in Los Angeles (Jacobson 1999), but future trends in soil moisture are also not known.

Long term trends in O_3 concentrations are currently being studied by many researchers. The weight of preliminary evidence suggests that background O_3 concentrations will increase from approximately 30 to 60 ppb in the next 50 to 100 years (Vingarzan 2004). In the current study, perturbations of background O_3 concentrations were chosen to simulate a doubling of global background O_3 concentrations to approximately 60 ppb.

5 Results

Figure 1a shows the predicted regional pattern of 1 h-average O_3 concentrations on September 9, 1993 at 15 PST. A band of high O_3 concentrations occurs along a line connecting Claremont, Riverside, and Perris, with the highest predicted concentrations reaching 290 ppb at Perris. Regional concentrations of O_3 over the entire modeling domain are large during the episode, approaching 90 ppb. Predicted O_3 concentrations in the region

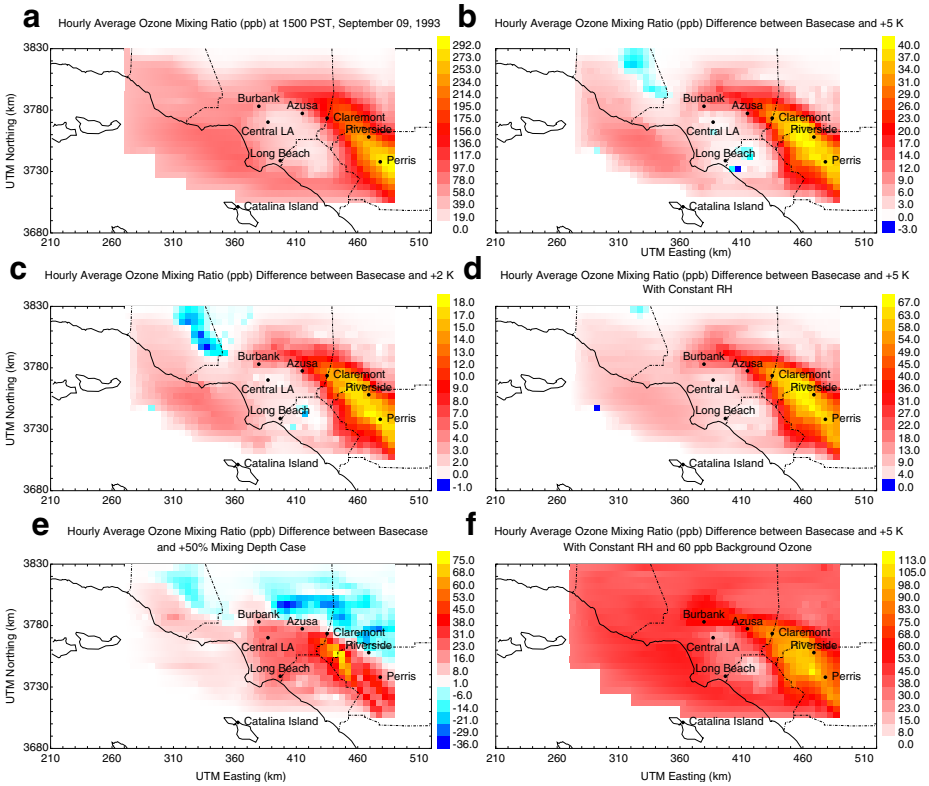

Fig. 1 Basecase O_3 concentration at 15 PST on September 9, 1993 (**a**) and sensitivity of O_3 concentration to **b** +5 K temperature change with constant absolute humidity, **c** +2 K temperature change with constant absolute humidity, **d** +5 K temperature change with constant relative humidity, **e** +50% increase in mixing depth, and **f** +5 K temperature change with constant relative humidity and increase in background O_3 from 30 to 60 ppb

immediately downwind of Central Los Angeles are slightly lower than the regional average because they are suppressed by emissions of fresh NO*x*.

Figure 1b and c show the predicted increase in regional O_3 concentrations at 15 PST on September 9, 1993 when temperature is uniformly perturbed at all times and locations by +5 K and +2 K, respectively. O_3 concentrations along the line connecting Claremont, Riverside, and Perris increase by approximately 18–40 ppb in response to this change. Regional O_3 concentrations at other locations increase by 4–14 ppb. Small regions with a ~1–3 ppb decrease are also observed, but these effects are minor compared to increases at other locations.

The underlying cause for the increase in O_3 concentrations at hotter temperatures can be diagnosed by looking at the speciation of nitrogen compounds. Table 4 shows the relative change to the concentration of O_3, hydroxyl radical (OH), total reactive nitrogen (RN), and various forms of reactive nitrogen at locations in the SoCAB at 15 PST on September 9, 1993 in response to a +5 K temperature perturbation. O_3 concentrations at these locations increase by 3–22% in response to the temperature change. The locations with the largest increase in O_3 concentrations (in the eastern end of the SoCAB) also have significant increases in hydroxyl radical (OH) concentrations. OH reacts with NO to form HONO. HONO further reacts with OH to form NO_2 or it can decomposes in the presence of sunlight to yield 90% NO and 10% NO_2. The net decrease in HONO concentrations evident in Table 4 suggests that the reaction with OH is more significant. Under either scenario, the enhanced OH concentrations convert NO to NO_2 leading to increased O_3 concentrations.

Large relative increases are observed in the concentration of nitrate radical (NO_3) at hotter temperatures, but NO_3 constitutes only a minor fraction of total reactive nitrogen. The concentration of nitric acid (HNO_3) is also enhanced at several locations when temperature is increased partially due to the reaction of increased OH concentrations with NO_2 and partly due to the evaporation of particulate nitrate (PN). All the reactive nitrogen species that undergo thermal decomposition reactions (N_2O_5, HNO_4, PAN, PN) have reduced concentrations at hotter temperatures as shown in Table 4. PAN concentrations summarize the net effect of all PAN-like species in the calculation. Many of these compounds decompose to form NO_2, but the resulting increase in NO_2 concentrations (−1 to +7%) is smaller than the decrease in NO concentrations (−6 to −21%) suggesting that the effect of increased hydroxyl radical concentrations is more significant than the thermal decomposition of various reactive nitrogen compounds. Total reactive nitrogen concentrations change by up to 6% because the different forms of reactive nitrogen have different loss rates.

Figure 1d shows the change in predicted regional O_3 concentrations at 15 PST on September 9, 1993 when temperature is uniformly perturbed by +5 K with no change to relative humidity. Basecase inland absolute humidity concentrations at 15 PST are on the

Table 4 Relative change in composition for O_3 (O_3), hydroxyl radical (OH), total reactive nitrogen (RN), and various forms of reactive nitrogen at 15 PST on September 9, 1993 caused by a +5 K temperature perturbation

	O_3	OH	RN	NO	NO_2	NO_3	N_2O_5	HONO	HNO_3	HNO_4	PAN	PN
LGBH	1.04	0.96	0.99	0.93	1.02	1.3	0.71	0.87	1.01	0.53	0.36	0.65
CELA	1.03	0.99	1.00	0.94	1.03	1.27	0.76	0.92	0.99	0.58	0.42	0.34
AZUS	1.22	1.20	0.97	0.79	1.01	1.80	0.86	0.93	1.04	0.84	0.76	0.38
CLAR	1.15	1.16	0.96	0.81	0.99	1.58	0.98	0.93	1.02	0.76	0.72	0.36
PERI	1.12	1.08	0.94	0.91	1.07	1.43	0.88	1.00	0.95	0.69	0.66	0.47

PN is particulate nitrate.

order of 15–20 ppth (parts per thousand) yielding relative humidity that ranges from 30–70%. When temperature is increased without adjusting absolute humidity, the relative humidity decreases. Given the proximity of the SoCAB to the Pacific Ocean, relative humidity may stay constant as temperature increases, leading to an effective increase in absolute humidity. The results in Fig. 1d can be compared to Fig. 1b which applied a +5 K temperature perturbation with no change to absolute humidity. The spatial distribution of increased O_3 concentrations shown in Fig. 1d matches that shown in Fig. 1b, but the magnitude of the predicted concentration increase is 67 ppb (vs. 40 ppb for the case with lower humidity). The increase in O_3 concentrations associated with higher concentrations of water vapor is caused by the production of hydroxyl radical from H_2O.

Figure 1e shows the change in predicted regional O_3 concentrations at 15 PST on September 9, 1993 in response to a uniform increase in mixing depths of +50%. The increased mixing depth leads to an increase in predicted O_3 concentrations in the western portion of the model domain by 75 ppb and a decrease in predicted O_3 concentrations in the eastern portion of the model domain by 36 ppb. Increased mixing depth reduces the concentration of primary pollutants such as oxides of nitrogen (NO*x*). Reduced NO*x* concentrations can promote higher O_3 concentrations in regions where there is an over abundance of NO*x*. The location of the maximum concentration increase differs slightly from the location of the predicted O_3 maximum in the base-case simulation, and so the net effect of the increased mixing depth is to slightly increase the maximum O_3 concentrations predicted during the episode and to increase the size of the region experiencing those maximum concentrations. The relationship between increased mixing depth and higher O_3 concentrations during severe photochemical episodes in the SoCAB has been noted previously during simulations of the Southern California Air Quality Study (SCAQS) [39].

Figure 1f shows the change in predicted regional O_3 concentrations at 15 PST on September 9, 1993 in response to a +5 K temperature perturbation with no changes to relative humidity when background O_3 concentrations are increased from 30 to 60 ppb. This result can be directly compared to Fig. 1d to view the effect of increased background O_3 concentrations. The additional 30 ppb of background O_3 increases regional O_3 concentrations by approximately 30 ppb but maximum O_3 concentrations are increased by approximately 46 ppb.

Figure 2a shows the predicted regional pattern of 24-h average $PM_{2.5}$ concentrations on September 9, 1993. The largest $PM_{2.5}$ concentration of 194 $\mu g\ m^{-3}$ is predicted to occur in the region west of Riverside where ammonia concentrations are very large leading to enhanced formation of particulate ammonium nitrate. The predicted concentration of $PM_{2.5}$ at most other locations in the inland portion of the modeling domain is 70–90 $\mu g\ m^{-3}$. The hot base-case temperatures during the current episode suppress the formation of large regions of particulate nitrate, since increasing temperature encourages nitrate evaporation (Aw and Kleeman 2003).

Figure 2b and c show the predicted change in regional $PM_{2.5}$ concentrations on September, 1993 when temperature is uniformly perturbed by +5 K and +2 K, respectively, at all times and locations. $PM_{2.5}$ concentrations in the region east of Riverside decrease by 14 to 31 $\mu g\ m^{-3}$ in response to this change. The majority of this reduction is associated with the volatilization of particulate ammonium nitrate as temperature increases. The location west of Riverside with the highest base-case concentration of particulate nitrate (see Fig. 2a) does not experience the largest reduction in $PM_{2.5}$ concentrations because regions with higher excess gas-phase ammonia concentrations respond less strongly to increased temperature than regions with lower excess gas-phase ammonia (Aw and Kleeman 2003). Figure 2b and c also show that regional average $PM_{2.5}$ concentrations are predicted

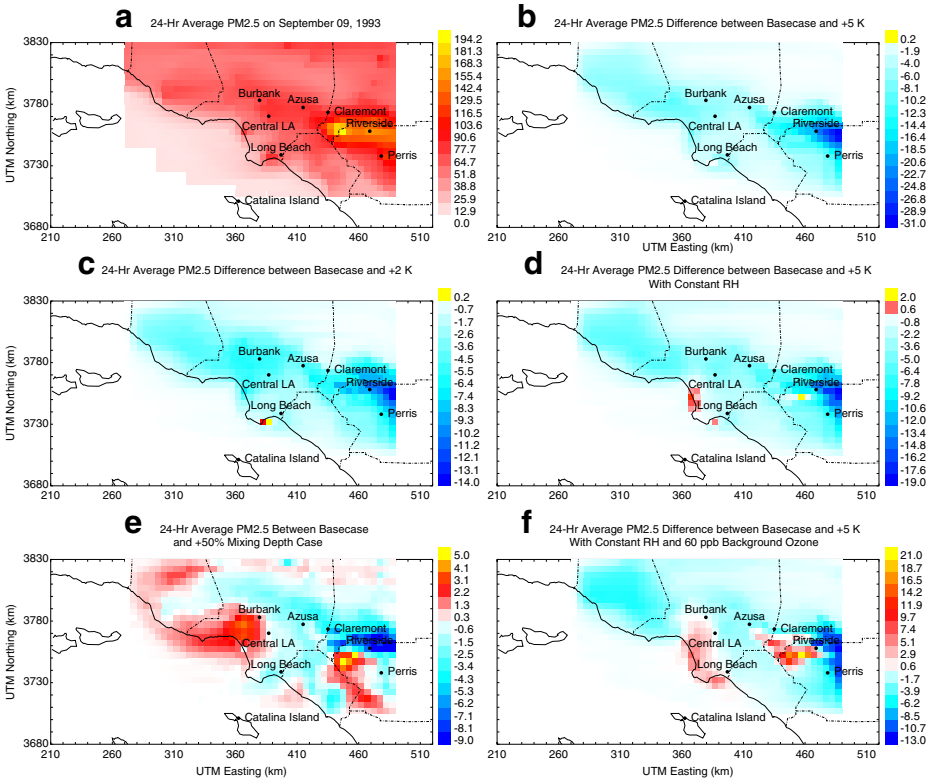

Fig. 2 Basecase $PM_{2.5}$ concentration on September 9, 1993 (**a**) and sensitivity of $PM_{2.5}$ concentration to **b** +5 K temperature change with constant absolute humidity, **c** +2 K temperature change with constant absolute humidity, **d** +5 K temperature change with constant relative humidity, **e** +50% increase in mixing depth, and **f** +5 K temperature change with constant relative humidity and increase in background O_3 from 30 to 60 ppb

to decrease by 3 to 15 μg m^{-3} in response to the +2 K and +5 K temperature perturbations. Once again, this change is caused by the partitioning of semi-volatile species to the gas phase at hotter temperatures, with particulate ammonium nitrate being the largest contributor to this effect. The region around the Long Beach harbor experiences a 0.2 μg m^{-3} increase in $PM_{2.5}$ concentrations in response to a +2 K temperature perturbation. Increased temperature promotes the oxidation of SO_2 emissions in this region to form sulfuric acid. Sulfur acid is essentially non-volatile at all ambient temperatures, and so this species partitions to the particle phase regardless of temperature perturbation.

Figure 2d shows the change in predicted regional $PM_{2.5}$ concentrations on September 9, 1993 when temperature is uniformly perturbed by +5 K with no changes to relative humidity. This figure can be compared to Fig. 2b which applied a +5 K temperature perturbation with no changes to absolute humidity. Maintaining relative humidity will maintain the amount of particle-phase water, leading to enhanced partitioning of water-soluble semi-volatile species. The reductions in particulate matter mass apparent in Fig. 2b are caused by the combined effect of increased temperature and reduced particle water content while the reductions in particulate matter mass shown in Fig. 2d are only caused by temperature. The region immediately west of Riverside experiences no decrease in $PM_{2.5}$ concentrations when temperature is increased by +5 K with no change to relative humidity, and one grid cell (5×5 km area) even experiences a 2 μg m^{-3} increase $PM_{2.5}$ concentra-

tions. The effect of temperature on particulate ammonium nitrate evaporation is moderated in regions with extremely high ammonia concentrations (Aw and Kleeman 2003). The area east of Riverside still experiences a decrease of $PM_{2.5}$ concentrations by approximately 19 μg m^{-3}, but this is moderated from the decrease of 36 μg m^{-3} predicted in the case with lower humidity. The reduction in regional average $PM_{2.5}$ concentrations in response to a +5 K increase in temperature is also moderated when relative humidity is maintained. Most inland regions experience a decrease in predicted $PM_{2.5}$ concentrations of 1 to 7 μg m^{-3}, with slight increases predicted in the region around the Long Beach Harbor, and the Los Angeles International Airport. The regional increases in $PM_{2.5}$ at these locations are once again associated with the enhanced production of sulfate aerosol from SO_2 emissions.

Figure 2e shows the change in predicted regional $PM_{2.5}$ concentrations on September 9, 1993 in response to a uniform increase in mixing depth of +50%. The maximum increase in $PM_{2.5}$ concentrations in response to this change is 5 μg m^{-3} in the region that experienced the largest increase in O_3 concentrations (see Fig. 1e). Predicted $PM_{2.5}$ concentrations in the region to the east of Riverside are reduced by 9 μg m^{-3} as the plume of enhanced nitrate is diluted by the increased mixing depth.

Figure 2f shows the change in predicted $PM_{2.5}$ concentrations on September 9, 1993 in response to a +5 K temperature perturbation with no change to relative humidity when background O_3 concentrations are increased from 30 to 60 ppb. This result can be directly compared to Fig. 2d to view the effect of increased background O_3 concentrations. Increased background O_3 concentrations lead to increased $PM_{2.5}$ concentrations through the production of additional particulate nitrate via the formation of N_2O_5 at night. The results illustrated in Fig. 2f show that a 30 ppb increase in background O_3 concentrations in the presence of a +5 K uniform temperature perturbation with no change to relative humidity leads to +5 to +8 μg m^{-3} increase in $PM_{2.5}$ concentrations near the Long Beach harbor and a +10 to +21 μg m^{-3} increase in $PM_{2.5}$ concentrations west of Riverside. Concentrations in other parts of the domain still decrease by −3 to –13 μg m^{-3} in the presence of the +5 K temperature perturbation (despite the increased background O_3).

Figures 3 and 4 illustrate the predicted effect of temperature, humidity, and mixing depth perturbations on O_3 and $PM_{2.5}$ concentrations in the SoCAB on September 25, 1996. The format used in Figs. 3 and 4 is identical to the format of Figs. 1 and 2. Figure 3a shows that the highest predicted 1 h-average O_3 concentration on September 25, 1996 at 15 PST is 120 ppb in the northeast corner of the domain that is downwind of the major emissions sources during this event. Concentrations immediately downwind of central Los Angeles are once again slightly lower than the regional average because they are suppressed by emissions of fresh NO*x*. Maximum predicted O_3 concentrations in this region are 70–80 ppb. Figure 4a shows that the largest basecase 24-h average $PM_{2.5}$ concentrations of 125 μg m^{-3} are predicted to occur in the region west and northeast of Riverside where ammonia concentrations are very large leading to enhanced formation of particulate ammonium nitrate. The predicted concentration of $PM_{2.5}$ at most other locations in the inland portion of the modeling domain is 40–80 μg m^{-3} on September 25, 1996. The moderate base-case temperatures during the current episode allow for the formation of significant quantities of particulate ammonium nitrate throughout the study region.

The predicted changes in O_3 and $PM_{2.5}$ concentrations in response to changes in meteorological variables and background O_3 is shown in Figs. 3b–f and 4b–f for September 25, 1996. In all cases, the qualitative behavior of O_3 and $PM_{2.5}$ on September 9, 1993 (Figs. 1 and 2) and September 25, 1996 (Figs. 3 and 4) are similar. Increased temperature results in higher predicted peak O_3 concentrations and lower predicted peak $PM_{2.5}$ concentrations (Figs. 3b, c and 4b, c). Increased humidity below the saturation

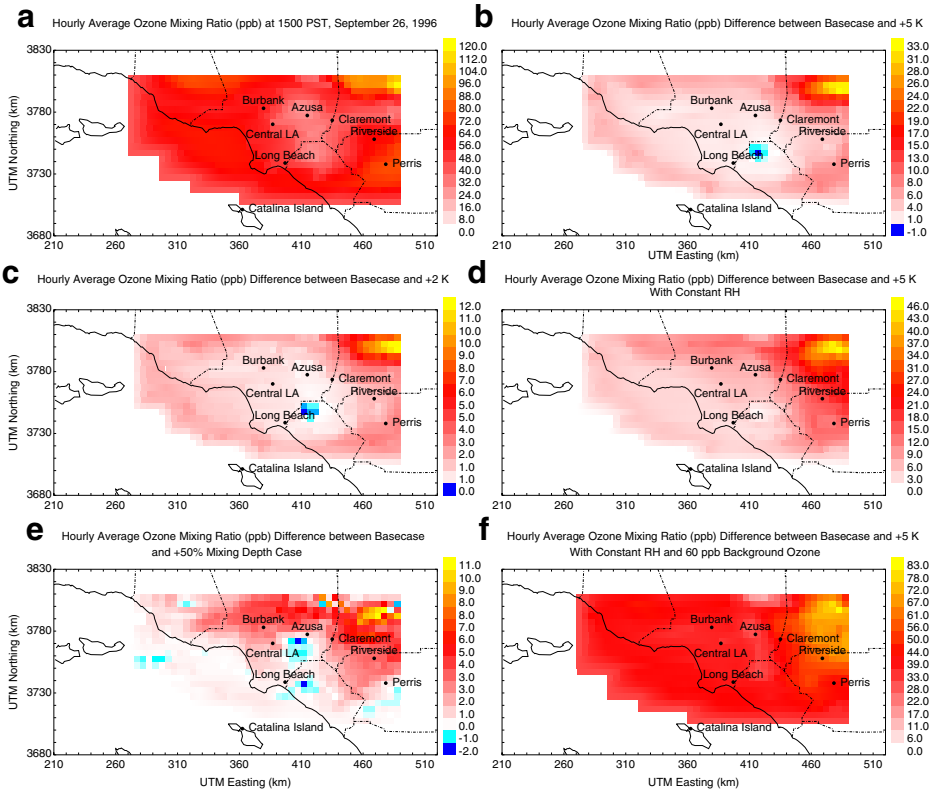

Fig. 3 Basecase O_3 concentration at 15 PST on September 25, 1996 (**a**) and sensitivity of O_3 concentration to **b** +5 K temperature change with constant absolute humidity, **c** +2 K temperature change with constant absolute humidity, **d** +5 K temperature change with constant relative humidity, **e** +50% increase in mixing depth, and **f** +5 K temperature change with constant relative humidity and increase in background O_3 from 30 to 60 ppb

threshold results in higher predicted peak O_3 and $PM_{2.5}$ concentrations (Figs. 3d and 4d). The magnitude of the positive humidity effect on $PM_{2.5}$ concentrations was generally smaller than the negative temperature effect. Increased mixing depth produced mixed results: O_3 and secondary $PM2_{2.5}$ increased in regions with excess NO while primary $PM_{2.5}$ and O_3 in regions without excess NO decreased (Figs. 3e and 4e). The magnitude of the effect caused by mixing depth was smaller on September 25, 1996 than September 9, 1993 because basecase mixing depths were larger during the 1996 episode. Increased background O_3 produced higher peak concentrations of O_3 and $PM_{2.5}$ inside the SoCAB (Figs. 3f and 4f). The magnitude of the positive effect on $PM_{2.5}$ caused by background O_3 was greater than the negative effect caused by a +5 K temperature perturbation.

Table 5 shows the relative change in O_3, hydroxyl radical (OH), total reactive nitrogen (RN), and various forms of reactive nitrogen in response to a +5 K temperature perturbation on September 25, 1996. The trends illustrated in Table 5 (September 1996) are similar to those shown in Table 4 (September 1993) but the magnitude of the changes are smaller. O_3 concentrations increase by 3–6%, largely due to a decrease in the concentration of NO by 6–9%. The apparent cause for the decrease in NO concentrations is an increase in OH that favors the production of NO_2 and HNO_3.

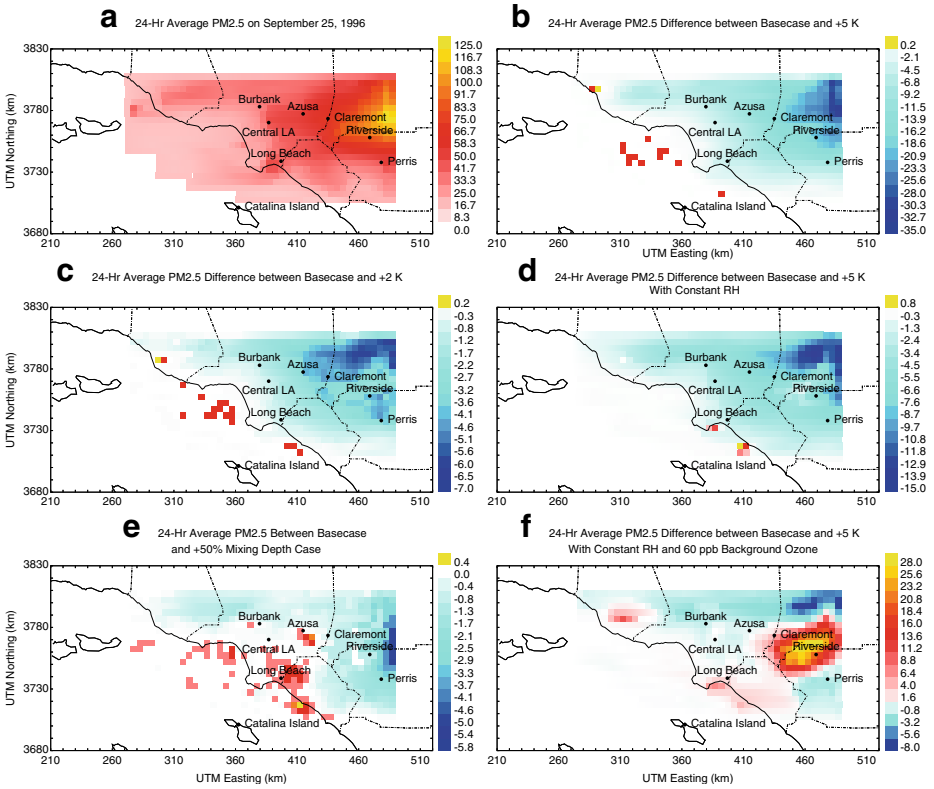

Fig. 4 Basecase $PM_{2.5}$ concentration on September 25, 1996 (**a**) and sensitivity of $PM_{2.5}$ concentration to **b** +5 K temperature change with constant absolute humidity, **c** +2 K temperature change with constant absolute humidity, **d** +5 K temperature change with constant relative humidity, **e** +50% increase in mixing depth, and **f** +5 K temperature change with constant relative humidity and increase in background O_3 from 30 to 60 ppb

Figure 5a shows the regional distribution of 1 h-average O_3 concentrations in the SJV at 1,500 PST on January 6, 1996. Peak O_3 concentrations are 41 ppb across a wide portion of the study domain except in regions with large NO*x* emissions where the O_3 concentrations are titrated to very low values. The O_3 suppression associated with the Highway 99 transportation corridor connecting Fresno, Visalia, and Bakersfield is clearly visible in this plot. Previous studies have noted that the excess NO*x* in the emissions inventory around Bakersfield appear to contradict measured concentrations in the region (Held et al. 2004).

Table 5 Relative change in composition for O_3 (O_3), hydroxyl radical (OH), total reactive nitrogen (RN), and various forms of reactive nitrogen at 15 PST on September 25, 1996 caused by a +5 K temperature perturbation

	O_3	OH	RN	NO	NO_2	NO_3	N_2O_5	HONO	HNO_3	HNO_4	PAN	PN
LGBH	1.03	0.89	0.99	0.94	1.02	1.25	0.68	0.87	1.07	0.47	0.31	0.78
CELA	1.03	1.03	0.98	0.91	1.01	1.29	0.69	0.92	1.13	0.57	0.47	0.64
AZUS	1.06	1.09	1.00	0.91	1.02	1.36	0.75	0.96	1.15	0.64	0.57	0.28
CLAR	1.06	1.11	1.02	0.92	1.03	1.36	0.75	0.98	1.20	0.65	0.61	0.26

PN is particulate nitrate.

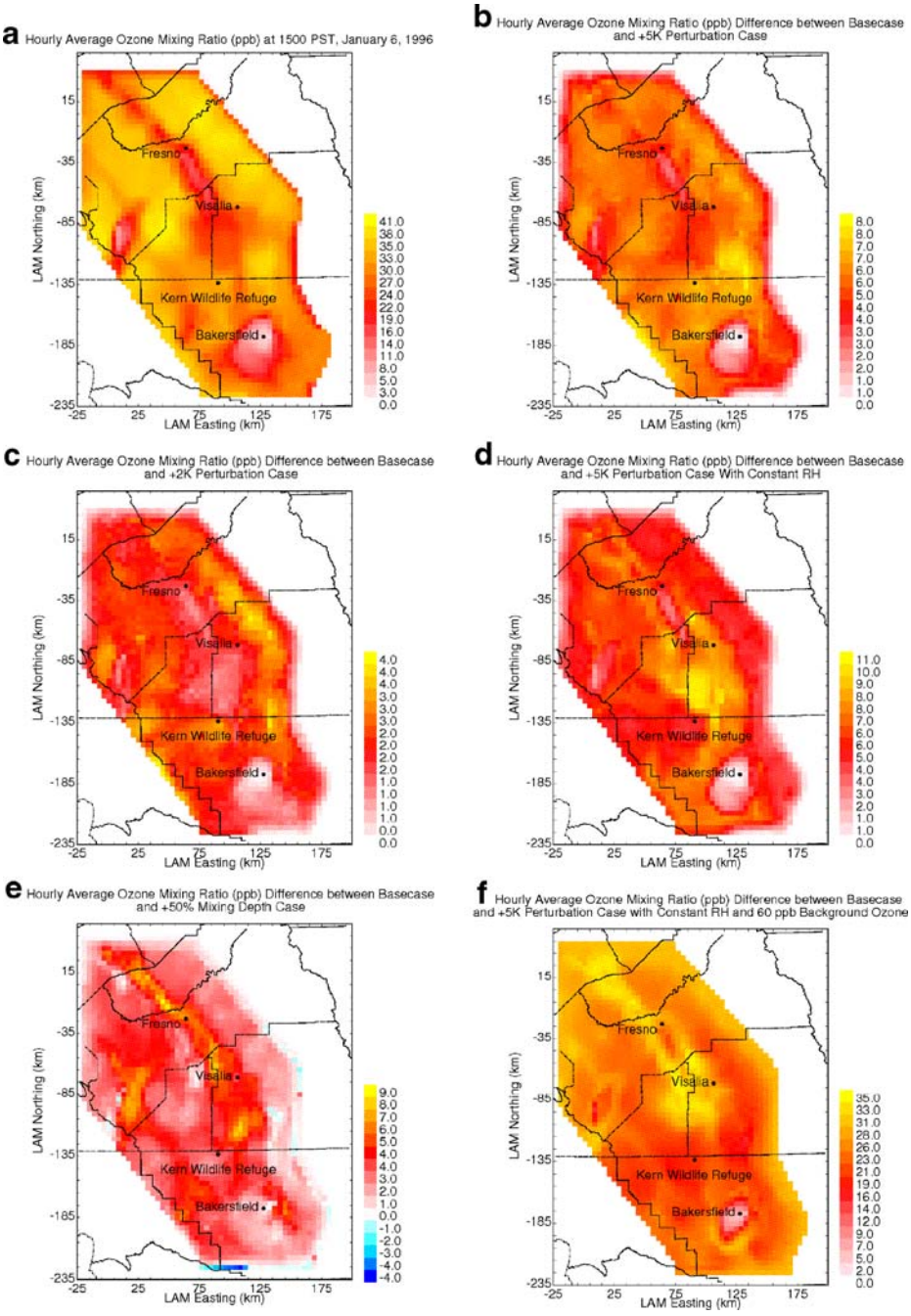

Fig. 5 Basecase O_3 concentration at 15 PST on January 6, 1996 (**a**) and sensitivity of O_3 concentration to **b** +5 K temperature change with constant absolute humidity, **c** +2 K temperature change with constant absolute humidity, **d** +5 K temperature change with constant relative humidity, **e** +50% increase in mixing depth, and **f** +5 K temperature change with constant relative humidity and increase in background O_3 from 30 to 60 ppb

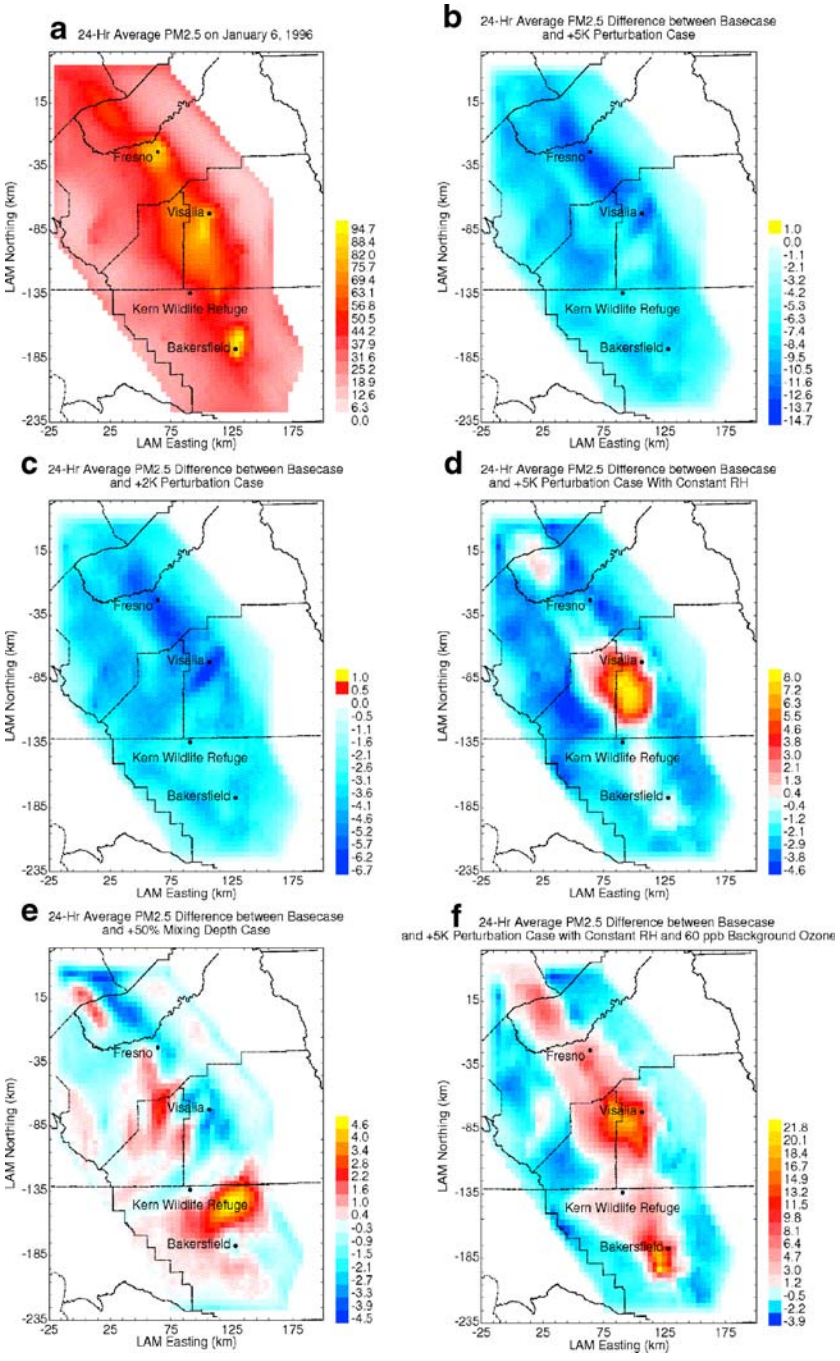

Fig. 6 Basecase $PM_{2.5}$ concentration on January 6, 1996 (**a**) and sensitivity of $PM_{2.5}$ concentration to **b** +5 K temperature change with constant absolute humidity, **c** +2 K temperature change with constant absolute humidity, **d** +5 K temperature change with constant relative humidity, **e** +50% increase in mixing depth, and **f** +5 K temperature change with constant relative humidity and increase in background O_3 from 30 to 60 ppb

Results in the area around Bakersfield are likely incorrect, but results for the remainder of the domain agree well with measurements and should be accurate. Figure 6a shows the regional distribution of 24-h average $PM_{2.5}$ concentrations in the SJV on January 6, 1996. Peak $PM_{2.5}$ values reach 95 μg m^{-3} around the urban locations of Fresno and Bakersfield due to the accumulation of wood smoke and other combustion particles combined with a regional background of ammonium nitrate particles peaking close to Visalia (Held et al. 2004).

Figure 5b–f illustrate the predicted change in O_3 concentrations in the SJV on January 6, 1996 in response to changes in meteorological parameters. The qualitative behavior of the SJV system shown in Fig. 5 matches the predicted behavior of the SoCAB illustrated in Figs. 1 and 3. Hotter temperatures enhance predicted local O_3 formation (Fig. 5b, c) as does increased humidity below the saturation threshold (Fig. 5d). Increased mixing depths produces higher O_3 concentrations in regions with transportation corridors that have an excess of fresh NO emissions (Fig. 5e). Higher concentrations of background O_3 directly increased the O_3 concentrations within the SJV (Fig. 5f).

Figure 6b–f illustrate the predicted change in $PM_{2.5}$ concentrations in the SJV on January 6, 1996 when meteorology is perturbed. Once again, the qualitative behavior of the SJV system is similar to that observed in the SoCAB (compare Fig. 6 with Figs. 2 and 4). Hotter temperatures reduce predicted $PM_{2.5}$ concentrations due to the evaporation of NH_4NO_3 (Fig. 6b, c) The region immediately south of Visalia does not experience a large decrease in $PM_{2.5}$ concentrations because NH_3 emissions in this region are very large, reducing the sensitivity of NH_4NO_3 to temperature. Increased humidity acted in the opposite direction as temperature because higher humidity increased the liquid water content of airborne particles which in turn promoted particulate NH_4NO_3 formation. Maintaining RH in the presence of a +5 K temperature perturbation produced increased $PM_{2.5}$ concentrations in the region with the highest NH_3 emissions (Fig. 6d). In the region immediately south of Visalia, an 8 μg m^{-3} increase in $PM_{2.5}$ concentrations is predicted to occur when relative humidity is constant and temperature increases by 5 K. The base temperature is low in the winter conditions during the current study, reducing the sensitivity of ammonium nitrate to temperature increases. The increase of temperature south of Visalia increases the formation rate of nitric acid faster than it increases the volatility of ammonium nitrate aerosol, leading to higher predicted $PM_{2.5}$ concentrations. It should be noted that the location of the maximum increase is slightly south of the maximum base-case concentrations. The net effect of this temperature increase is to expand the region of maximum $PM_{2.5}$ concentrations during the current study. Other locations in the SJV with lower amounts of excess gas-phase ammonia experience a decrease in $PM_{2.5}$ concentrations of 4.6 μg m^{-3} in response to a +5 K temperature perturbation even when relative humidity remains constant.

Table 6 shows the relative change in O_3, hydroxyl radical (OH), total reactive nitrogen (RN), and various forms of reactive nitrogen in response to a +5 K temperature perturbation on January 6, 1996. Once again, the increased temperature changes the speciation of reactive nitrogen, leading to decreased concentrations of NO and increased concentrations of NO_2. O_3 concentrations at Fresno (FEI) and Kern Wildlife Refuge (KWR) both increase by 19%, but at Fresno the change is largely driven by a decrease in NO while at Kern Wildlife Refuge the change is largely driven by an increase in NO_2 concentrations. This difference in behavior is likely caused by the fact that Fresno is an urban city while Kern Wildlife Refuge is a remote location. The fresh emissions at the urban location result in behavior that matches the trends observed in the South Coast Air Basin (see Tables 4 and 5).

Table 6 Relative change in composition for O_3 (O_3), hydroxyl radical (OH), total reactive nitrogen (RN), and various forms of reactive nitrogen at 15 PST on January 6, 1996 caused by a +5 K temperature perturbation

	O_3	RN	NO	NO_2	NO_3	N_2O_5	HONO	HNO_3	HNO_4	PAN	PN
FEI	1.19	1.00	0.83	1.05	1.73	0.96	0.87	1.59	0.73	0.62	0.23
KWR	1.19	1.01	0.96	1.23	1.75	1.17	1.09	3.64	0.75	0.72	0.88

PN is particulate nitrate.

Figure 6e shows the change in predicted regional $PM_{2.5}$ concentrations on January 6, 1996 in response to a uniform increase in mixing depths of +50%. Predicted $PM_{2.5}$ concentrations immediately north of Bakersfield increase by +4.6 μg m^{-3} in response to the increased mixing depth because the diluted NO*x* concentrations form more nitric acid which interacts with the ammonia plume just north of that location. As noted previously, the high NO*x* emissions in the Bakersfield region are an artifact of the emissions inventory used in the current study, and so this increase in concentrations is likely also an artifact. $PM_{2.5}$ concentrations at locations farther north in the domain are predicted to undergo slight decreases or increases associated with the enhanced mixing of pollutants aloft to the surface.

Figure 6f shows the change in predicted regional $PM_{2.5}$ concentrations on January 6, 1996 when background O_3 concentrations are increased from 30 to 60 ppb while temperature is uniformly increased by 5 K with no changes in relative humidity. The formation of particulate nitrate via the nighttime reaction of N_2O_5 is particularly important during winter SJV episodes, and so the $PM_{2.5}$ concentrations respond strongly to background O_3. The entire central portion of the study domain is predicted to experience a +5 to +20 μg m^{-3} increase in $PM_{2.5}$ concentrations under these conditions. The largest increase occurs near Visalia where ammonia concentrations are large.

6 Discussion

Figure 7 summarizes the range of changes in predicted O_3 and $PM_{2.5}$ concentrations resulting from all the meteorological perturbations considered in the current study when background O_3 concentrations are set equal to 60 ppb (approximately double present-day conditions). The bars shown in Fig. 7 illustrate the largest change in pollutant concentrations predicted anywhere in the domain, while the circles illustrate the change in the maximum concentrations. When the circles are located close to the extreme values of the bars, it shows that the greatest change in concentration occurs at the location of maximum concentration.

Figure 7 shows that increasing temperature with no change in absolute humidity generally increases peak O_3 concentrations in all the episodes studied. $PM_{2.5}$ concentrations decrease in some parts of the study domain, but peak concentrations generally increase during all of the episodes studies, largely because the temperature effect (reducing $PM_{2.5}$ formation) is overwhelmed by the effect of background O_3 (promoting $PM_{2.5}$ formation). Increasing temperature with no change to relative humidity increases predicted O_3 concentrations even further due to the enhanced production of hydroxyl radical. The increased humidity also mitigates the reduction in $PM_{2.5}$ concentrations leading to greater increases, especially in the SJV in regions with large excesses of gas-phase ammonia and cooler basecase temperatures.

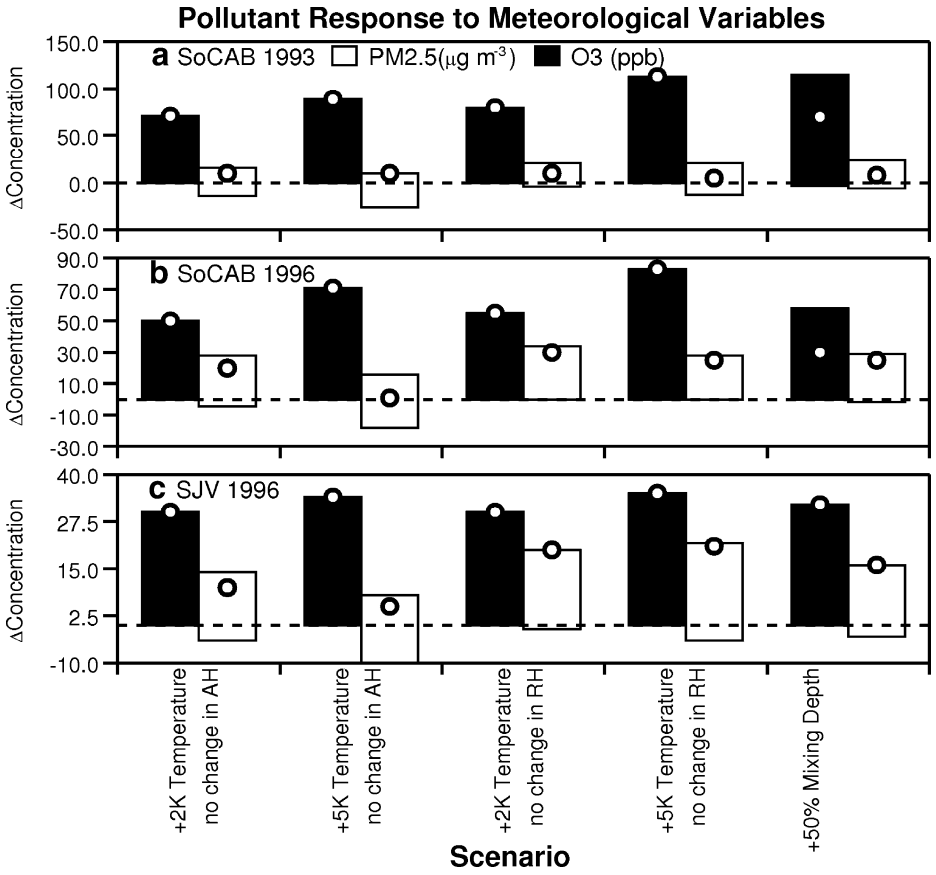

Fig. 7 Summary of pollutant response to meteorological perturbations when background O_3 concentrations are 60 ppb during pollution episodes that occurred in **a** Southern California September 9, 1993, **b** Southern California September 25, 1996, and **c** the San Joaquin Valley January 6, 1996. The *bars* represent the range of concentration change at any location in the modeling domain in response to the indicated perturbation. The *circles* represent the concentration change at the location of the maximum concentration for each pollutant. AH is absolute humidity and RH is relative humidity

Figure 7 generally shows that increasing mixing depths usually increases surface O_3 concentrations because the extra volume allows for increased dilution of fresh NO*x* emissions, reducing the titration of surface O_3 concentrations. This effect may not be significant at the location of maximum O_3 concentration. The increased mixing depth also usually reduces primary $PM_{2.5}$ concentrations through increased dilution. Secondary $PM_{2.5}$ can increase as mixing depth rises due to the same chemistry that enhances O_3 formation under these conditions. The effect of mixing depth on $PM_{2.5}$ concentrations is generally smaller than the effect of background O_3, which promotes enhanced $PM_{2.5}$ concentrations.

Emissions of NO*x*, VOC, and particulate matter in California have been reduced over the last several decades in an attempt to control ambient O_3 and airborne particulate matter concentrations to protect public health. The emissions totals summarized in Table 3 for the SoCAB reflect the predicted effects of emissions control programs between 1993 and 1996. Similar downward emissions trends are predicted for the SJV. The effectiveness of future emissions control programs will be determined by the competition between projected

increases in population vs. improved efficiency or other technological advances that reduce emissions per unit of activity. Even if emissions are reduced to levels that achieve the National Ambient Air Quality Standards (NAAQS), meteorology will still affect air pollutant concentrations in California. The SJV already has significantly lower emissions than the SoCAB and the predicted response of O_3 and $PM_{2.5}$ to changes in temperature, humidity, and mixing depth in the SJV are qualitatively similar to those in the SoCAB. The results of the present analysis suggest that meteorological conditions that enhance the formation of O_3 and $PM_{2.5}$ will require stricter emissions control programs than would otherwise have been required to achieve the NAAQS. Further research is needed to quantify the magnitude of this effect.

7 Conclusions

The trends illustrated in the previous section show that air pollution problems in California are sensitive to temperature, humidity, mixing depth, and background concentrations. Future trends for temperature, humidity, mixing depth, and background concentrations are not exactly known at this time, but the weight of scientific evidence suggests that background O_3 concentrations and temperature are likely to rise. The results of the current study suggest that these changes will lead to increased O_3 concentrations in California.

The $PM_{2.5}$ response to global change is more complicated to diagnose because some of the likely trends act in opposite directions. Increased temperature discourages the formation of particulate ammonium nitrate, but rising concentrations of background O_3 encourages the formation of this same species. $PM_{2.5}$ concentrations increased in all of the episodes currently studied under the limiting scenario of a +5 K temperature increase with no change in absolute humidity and a +30 ppb increase in background O_3. The effect of increased background O_3 was especially important during episodes with lower basecase temperatures. $PM_{2.5}$ events in the San Joaquin Valley usually occur during the winter months, and so increased background O_3 concentrations have a strong positive effect on $PM_{2.5}$ concentrations in this location. These results suggest that global change will increase $PM_{2.5}$ concentrations in California, but more research is needed to verify this result.

Acknowledgment This research was funded by the California Air Resources Board under Contract # 04-349. The statements and conclusions of this Report are those of the contractor and not necessarily those of the California Air Resources Board. The mention of commercial products, their source, or their use in connection with material reported herein is not to be construed as actual or implied endorsement of such products.

References

Aw J, Kleeman MJ (2003) Evaluating the first-order effect of intraannual temperature variability on urban air pollution. J Geophys Res – Atmospheres 108(D12)4365

Carter WPL (1990) A detailed mechanism for the gas-phase atmospheric reactions of organic-compounds. Atmos Environ, A Gen Topics 24(3):481–518

Duffy PB, Arritt RW, Coquard J, Gutowski W, Han J, Iorio J, Kim J, Leung LR, Roads J, Zeledon E (2006) Simulations of present and future climates in the western United States with four nested regional climate models. J Climate 19(6):873–895

Fraser MP, Kleeman MJ, Schauer JJ, Cass GR (2000) Modeling the atmospheric concentrations of individual gas-phase and particle-phase organic compounds. Environ Sci Technol 34(7):1302–1312

Fredenslund A, Gmehling J, Rasmussen P (1977) Vapor–liquid equilibrium using UNIFAC. Elsevier, New York
Griffin RJ, Dabdub D, Seinfeld JH (2002a) Secondary organic aerosol – 1. Atmospheric chemical mechanism for production of molecular constituents. J Geophys Res – Atmospheres 107(D17)
Griffin RJ, Dabdub D, Kleeman MJ, Fraser MP, Cass GR, Seinfeld JH (2002b) Secondary organic aerosol 3. Urban/regional scale model of size- and composition-resolved aerosols. J Geophys Res – Atmospheres 107(D17):AAC5/1–AAC5/14
Griffin RJ, Dabdub D, Seinfeld JH (2005) Development and initial evaluation of a dynamic species-resolved model for gas phase chemistry and size-resolved gas/particle partitioning associated with secondary organic aerosol formation. J Geophys Res 110(D5)
Held T, Ying Q, Kaduwela A, Kleeman M (2004) Modeling particulate matter in the San Joaquin Valley with a source-oriented externally mixed three-dimensional photochemical grid model. Atmos Environ Part, A Gen Topics 38(22):3689–3711
Held AE, Ying Q, Kleeman MJ, Schauer JJ, Fraser MP (2005) A comparison of the UCD/CIT air quality model and the CMB source-receptor model for primary airborne particulate matter. Atmos Environ Part, A Gen Topics 39:2281–2297
Hogrefe C, Lynn B, Civerolo K, Ku JY, Rosenthal J, Rosenzweig C, Goldberg R, Gaffin S, Knowlton K, Kinney PL (2004) Simulating changes in regional air pollution over the eastern United States due to changes in global and regional climate and emissions. J Geophys Res 109(D22)
Houghton JT et al. (ed) 2001 Climate change: the scientific basis. Contribution of working group I to the third assessment report of the Intergovernmental Panel on Climate Change (IPCC). Cambridge University Press, Cambridge.
Jacobson MZ (1999) Effects of soil moisture on temperatures, winds, and pollutant concentrations in Los Angeles. J Appl Meteorol 38(5):607–616
Kim BM, Teffera S, Zeldin MD (2000) Characterization of PM2.5 and PM10 in the South Coast Air Basin of southern California: Part 1 – Spatial variations. J Air Waste Manage Assoc 50(12):2034–2044
Kleeman MJ, Cass GR (2001) A 3D Eulerian source-oriented model for an externally mixed aerosol. Environ Sci Technol 35(24):4834–4848
Kleeman MJ, Cass GR, Eldering A (1997) Modeling the airborne particle complex as a source-oriented external mixture. J Geophys Res – Atmospheres 102(Sep 20):21355–21372
Kleeman MJ, Hughes LS, Allen JO, Cass GR (1999) Source contributions to the size and composition distribution of atmospheric particles: Southern California in September 1996. Environ Sci Technol 33 (23):4331–4341
Kleeman MJ, Ying Q, Kaduwela A (2005) Control strategies for the reduction of airborne particulate nitrate in California's San Joaquin Valley. Atmos Environ 39(29):5325–5341
Klonecki A, Levy H (1997) Tropospheric chemical ozone tendencies in CO-CH4-NOy-H2O system: their sensitivity to variations in environmental parameters and their application to a global chemistry transport model study. J Geophys Res 102(D17):21221–21237
Kusik CL, Meissner HP (1978) Electrolyte activity coefficients in inorganic processing. Fund Asp Hydrometallurgical Processes AIChE Symposium Series 74:14–20
Langner J, Bergstrom R, Foltescu V (2005) Impact of climate change on surface ozone and deposition of sulphur and nitrogen in Europe. Atmos Environ 39(6):1129–1141
Leung LR, Qian Y, Bian XD, Washington WM, Han JG, Roads JO (2004) Mid-century ensemble regional climate change scenarios for the western United States. Clim Change 62(1–3):75–113
Liao H, Chen WT, Seinfeld JH (2006) Role of climate change in global predictions of future tropospheric ozone and aerosols. J Geophys Res 111:D12304
Mickley LJ, Jacob DJ, Field BD, Rind D (2004) Effects of future climate change on regional air pollution episodes in the United States. Geophys Res Lett 31(24):L24103
Murazaki K, Hess P (2006) How does climate change contribute to surface ozone change over the United States? J Geophys Res 111(D5)
Mysliwiec MJ, Kleeman MJ (2002) Source apportionment of secondary airborne particulate matter in a polluted atmosphere. Environ Sci Technol 36(24):5376–5384
Odum JR, Hoffmann T, Bowman F, Collins D, Flagan RC, Seinfeld JH (1996) Gas/particle partitioning and secondary organic aerosol yields. Environ Sci Technol 30(8):2580–2585
Pandis SN, Harley RA, Cass GR, Seinfeld JH (1992) Secondary organic aerosol formation and transport. Atmos Environ, A Gen Topics 26(13):2269–2282
Prather M, Gauss M, Berntsen T, Isaksen I, Sundet J, Bey I, Brasseur G, Dentener F, Derwent R, Stevenson D, Grenfell L, Hauglustaine D, Horowitz L, Jacob D, Mickley L, Lawrence M, von Kuhlmann R, Muller JF, Pitari G, Rogers H, Johnson M, Pyle J, Law K, van Weele M, Wild O (2003) Fresh air in the 21st century? Geophys Res Lett 30(2)
Pun BK, Griffin RJ, Seigneur C, Seinfeld JH (2002) Secondary organic aerosol – 2. Thermodynamic model for gas/particle partitioning of molecular constituents. J Geophys Res – Atmospheres 107(D17)

Sillman S, Samson FJ (1995) Impact of temperature on oxidant photochemistry in urban, polluted rural and remote environments. J Geophys Res 100(D6):11497–11508

VanCuren RA, Cahill TA (2002) Asian aerosols in North America: frequency and concentration of fine dust. J Geophys Res 107(D24)

Vingarzan R (2004) A review of surface ozone background levels and trends. Atmos Environ 38(21):3431–3442

Ying Q, Kleeman MJ (2006) Source contributions to the regional distribution of secondary particulate matter in California. Atmos Environ 40(4):736–752

Ying Q, Kleeman M (2007) Verification of a source-oriented external mixture air quality model during a severe photochemical smog event. Atmos Environ, A Gen Topics 41:1521–1538